

Direct monitoring of porosity evolution by dynamic modulus measurements: Three case studies

Marcello Cabibbo, Chiara de Crescenzo, Roberto Montanari, Maria Richetta & Alessandra Varone

To cite this article: Marcello Cabibbo, Chiara de Crescenzo, Roberto Montanari, Maria Richetta & Alessandra Varone (2023) Direct monitoring of porosity evolution by dynamic modulus measurements: Three case studies, European Journal of Materials, 3:1, 2208159, DOI: [10.1080/26889277.2023.2208159](https://doi.org/10.1080/26889277.2023.2208159)

To link to this article: <https://doi.org/10.1080/26889277.2023.2208159>



© 2023 The Author(s). Published by Informa UK Limited, trading as Taylor & Francis Group.



Published online: 10 May 2023.



Submit your article to this journal [↗](#)



Article views: 69



View related articles [↗](#)



View Crossmark data [↗](#)

Direct monitoring of porosity evolution by dynamic modulus measurements: Three case studies

Marcello Cabibbo^a, Chiara de Crescenzo^b, Roberto Montanari^b, Maria Richetta^b and Alessandra Varone^b

^aDipartimento di Ingegneria Industriale e Scienze Matematiche (DIISM), Università Politecnica delle Marche, Ancona, Italy; ^bDipartimento di Ingegneria Industriale, Università di Roma "Tor Vergata", Roma, Italy

ABSTRACT

Porous materials are playing an increasingly relevant role in several fields and industrial sectors with structural and functional applications. Their properties critically depend on the relative density and pore morphology thus it is of great importance monitoring the variations of such structural features. Among the experimental techniques commonly used for investigating the microstructure evolution of porous materials, Mechanical Spectroscopy (MS) provides damping and dynamic modulus of the material during heat treatments. In this work three cases of possible pore structure evolution in different metallic alloys have been examined by MS: (i) growth and coalescence of pores, (ii) closure of pores of nanometric size and (iii) no change of porosity.

The results show how dynamic modulus measurements can be successfully employed for a direct monitoring of porosity variations during heating. The technique is quite sensitive and allows to identify the temperature range where pore evolution takes place providing information useful to orientate heat treatments of porous materials.

ARTICLE HISTORY

Received 12 January

2023

Accepted 23 April 2023

KEYWORDS

Porous metals;
mechanical spectroscopy;
dynamic modulus

CONTACT Roberto Montanari  roberto.montanari@uniroma2.it  Dipartimento di Ingegneria Industriale e Scienze Matematiche (DIISM), Università Politecnica delle Marche, Via Brecce Bianche 12, 60131 Ancona, Italy.

© 2023 The Author(s). Published by Informa UK Limited, trading as Taylor & Francis Group. This is an Open Access article distributed under the terms of the Creative Commons Attribution License (<http://creativecommons.org/licenses/by/4.0/>), which permits unrestricted use, distribution, and reproduction in any medium, provided the original work is properly cited. The terms on which this article has been published allow the posting of the Accepted Manuscript in a repository by the author(s) or with their consent.

1. Introduction

Thanks to their unique combination of properties, porous materials (metals, ceramics and polymers) are playing an increasingly relevant role in several fields and industrial sectors including aerospace, chemical, energy, electronics, transportation and biomedical (Michailidis, Tsouknidas, Lefebvre, Hipke, & Kanetake, 2014), with structural and functional (Vijayan, Anna Dilfi, & Venkatachalapathy, 2022) applications. Therefore, they have received a great deal of technological and scientific attention mainly focused on the development of novel fabrication methods to control the pore structure from nano- to macro-scale (Dukhan, Chen-Wiegart, Paz y Puente, Erdeniz, & Dunand, 2020; Yang et al., 2017) and consequently their physico-chemical properties (e.g. see Bennett, Coudert, James, & Cooper, 2021; Nakajima, 2007; Sousa et al., 2023; Suzuki, Kosugi, Takata, & Kobashi, 2020). Recently, Additive Manufacturing (AM) has been also used to manufacture porous and lattice materials with various architectures (Jafari et al., 2020).

Mechanical and other properties of these materials are strongly affected by relative density, shape, strut thickness, size, and size distribution of pores, and significant changes may be induced by heat treatments, pressure, etc. thus it is of the utmost importance monitoring the variations of such structural features. The porosity can change in different ways: both closure of pores or growth of pores can be observed depending on the presence of gas, diffusive atomic motions, pressure and other factors.

There are a lot of experimental methods, both destructive and not destructive, commonly used for characterising porous and cellular materials: porosimetry, X-ray radiography and tomography, measurements of Eddy-current, acoustic response, electrical and thermal conductivity, analysis of images collected from light and electron microscopy and others (Banhart, 2001; Michailidis, Stergioudi, Omar, Papadopoulos, & Tsipas, 2011). Among them, Mechanical Spectroscopy (MS) provides damping and dynamic modulus under different conditions of temperature or strain.

Principles and applications of MS can be found in the book of Nowick and Berry (1972) while a literature data collection is reported in that of Blanter, Golovin, Neuhäuser, and Sinning (2007). MS is commonly employed for investigating physical phenomena occurring in materials but has been also used by present authors to study different problems of industrial interest, such as: (i) interstitial-substitutional atom interactions in martensitic steels for structural applications in future nuclear fusion reactors (Alberici, Montanari, & Tata, 2000; Bolli et al., 2020; Gondi & Montanari, 1992, 1994; Gupta, Gondi, Montanari, Principi, & Tata, 1997), (ii) irreversible transformations occurring in FeAl B2-ordered alloy obtained by melt spinning (Bonetti, Montanari, Testani, & Valdré,

2000), (iii) damping of Ti6Al4V + SiC_f composite (Amadori et al., 2009; Deodati, Donnini, Montanari, & Testani, 2009) and superalloys for aeronautic applications (Deodati, Donnini, et al., 2009), (iv) precursor phenomena of melting in alloys (Montanari & Varone, 2012) and pure metals (Montanari & Varone, 2015), (v) mechanical behaviour of Oxide Dispersion Strengthened (ODS) steels (Fava, Montanari, Richetta, Testani, & Varone, 2018), and (vi) anelastic behaviour of Al thin foils for MEMS applications (Bonetti, Cabibbo, Campari, & Montanari, 2021; Campari, Amadori, Bonetti, Berti, & Montanari, 2019).

Relationships between elastic modulus and density found in literature are quite various. In addition to some empirical equations, there are a lot of analytic treatments where pores are modelled by using different geometrical shapes such as cylinders (Eudier, 1962), rectangular parallelepipeds (Bocchini, Montanari, & Varone, 2013), 3D arrangement of connected beams (Gibson & Ashby, 1989) and spheroids (e.g. see Boccaccini, Ondracek, Mazilu, & Windelberg, 1993; Chen, Wang, Giuliani, & Atkinson, 2015; Kovačik, 1999; Manoylov, Borodich, & Evans, 2013; Pabst & Gregorová, 2014; Torquato, 2002). Indeed, today a general theory of pore shape effects is out of sight, even if some structures can be treated analytically. The matter has been already extensively discussed in Richetta and Varone (2020).

This work discusses the possibility to use MS to get a direct monitoring of the porosity change following heat treatments. In particular, dynamic modulus, that is strictly connected to the density of the material, allows to detect with high sensitivity possible variations of the pore structure. To illustrate the application of the technique, three typical cases of different materials have been examined:

- i. growth and coalescence of pores in the nanostructured Fe-1.5 wt.% Mo alloy prepared by Spark Plasma Sintering (SPS),
- ii. closure of pores of nanometric size in AlSi10Mg alloy manufactured by Laser Powder Bed Fusion (L-PBF),
- iii. no change of porosity in the Ti6Al4V alloy manufactured by L-PBF.

The selected cases have been chosen because they are considered relevant and representative of different situations.

2. Dynamic modulus measurements

The elastic modulus of a material depends on the strength of interatomic bonds that cannot be altered by the presence of pores, however dynamic modulus E measured in present experiments is the effective modulus.

The tests were carried out by means of the automated vibrating reed analyzer (VRA 1604, CANTIL s.r.l, Bologna, Italy) described in detail in Amadori et al. (2006). Bar-shaped probes ($28\text{ mm} \times 7\text{ mm} \times 0.46\text{ mm}$) were mounted in cantilever and excited by flexural vibrations. The measurements were made in conditions of resonance with resonance frequency f in the range of kHz, under a 10^{-6} mbar pressure and at a strain amplitude of $\sim 10^{-6}$.

A single electrode was used to excite and reveal the probe vibrations. As shown in Figure 1, to excite the vibrations, the electrode is parallel to the probe and a periodic voltage is applied while for the detection a capacitive method is used. The experimental apparatus automatically identifies the response frequency and follows it while it changes, e.g. during heating. The tests were performed by increasing the temperature with a heating rate of $1^\circ\text{C}/\text{min}$.

Dynamic modulus E has been calculated from the resonance frequency f by means of the relationship:

$$E = \left(\frac{2\pi\sqrt{12}}{m^2} \right)^2 f^2 \rho \frac{L^4}{h^2} \Omega \quad (1)$$

where ρ is the density of the material, m is a constant depending on the vibration mode, L and h are the length and thickness of the probe, respectively. Ω is a geometrical correction factor given by:

$$\Omega = 1.000 + 6.585 \left(\frac{h}{L} \right)^2 \quad (2)$$

that becomes ≈ 1 if $L/h > 20$. In present tests the first vibration mode was used thus $m = 1.875$ while $\Omega = 1$ because of the dimensions of probes ($L/h \cong 60$).

In MS experiments porosity evolution involves a change of material density consisting in a volume change because the mass of the sample remains constant. In a sample without any porosity material density and

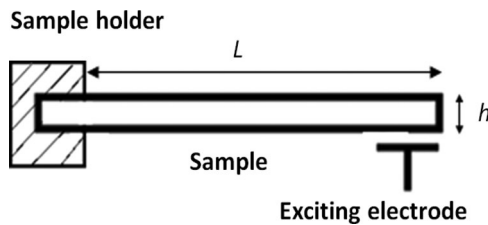


Figure 1. Schematic view of the reed mounted in free-clamped mode and the electrode exciting the flexural vibrations.

sample dimensions change due to thermal expansion during the heating part of a test run and modulus progressively decreases. The opposite occurs during the cooling part of the cycle. When a single test run has been completed the values of density, dimensions and modulus are the original ones. The behaviour of a porous material is the same if porosity does not change. If a change of porosity occurs at the end of the test run there are permanent variations of density, dimensions and modulus. In the case of a random distribution of pores the three dimensions of the sample vary uniformly.

3. Results and discussion

3.1 Pore growth and coalescence in nanostructured Fe-1.5 wt.% Mo alloy prepared by SPS

The investigated material was the Fe-1.5 wt.% Mo alloy. It was prepared by SPS of powders treated by high energy ball milling to induce the nanostructure and then mixed with 1.5 wt.% of SiO₂ powders (mean size ~10 nm) to hinder grain growth. A DR.SINTER® SPS1050 (Sumitomo Coal & Mining, now SPS SyntexInc.) apparatus with graphite punches and die has been used for SPS process through the following steps: heating at 1.7°C/s up to 840°C by applying a pressure of 30 MPa, holding for 60s and free cooling. More details are reported in Mitchell et al. (2008).

From the disks produced by SPS (diameter = 30 mm, height = 5 mm) were cut the reeds for MS tests. MS experiments consisted of successive test runs carried out on the same sample and each run was a heating-cooling cycle starting from room temperature (25°C) to 650°C. The measurements have been repeated on 15 different samples in the same experimental conditions.

Discs for Transmission Electron Microscopy (TEM) inspections were prepared by using a Precision Ion Polishishing System (PIPS) ion miller. Thin foils were mechanically ground to 100–120 µm, punched and dimpled down to a thickness ranging 30–35 µm. Ion milling was initially set to a voltage of 5 V and a tilt angle of 4°, followed by the final step at a tilt angle of 2° while the sample holder was chilled through liquid nitrogen. TEM inspections were carried out using a Philips™ CM200 equipped with a double tilt specimen holder and images were recorded using a dedicated CCD camera.

Figure 2 shows the curves of dynamic modulus in the 1st and 2nd test runs on the same sample. Dynamic modulus values are normalized to E_0 , the modulus of the original material, determined from the initial resonance frequency ($f_0 = 1812$ Hz) through Eq. (1).

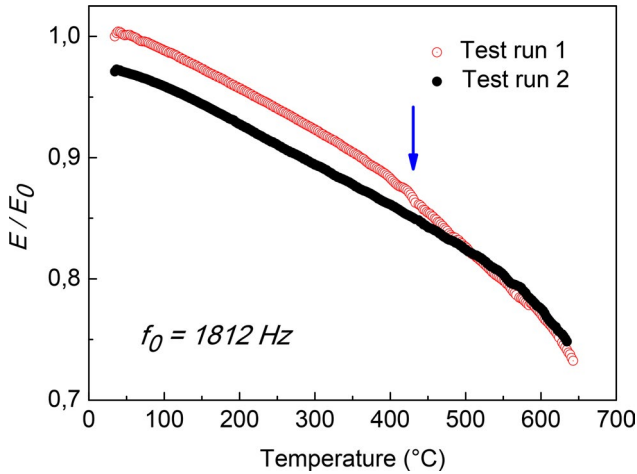


Figure 2. Dynamic modulus curves vs. temperature in the 1st and 2nd test runs on the same sample. Dynamic modulus values are normalized to E_0 , the modulus of the original material, determined from the initial resonance frequency ($f_0 = 1812 \text{ Hz}$).

In the 1st test run dynamic modulus monotonically decreases but at $\sim 430^{\circ}\text{C}$ exhibits a sudden slope change that is no more observed in successive test runs on the same sample. After the completion of the 1st test run dynamic modulus is $\sim 3\%$ lower than E_0 and this change corresponds to an irreversible transformation.

TEM micrographs in Figure 3 show at the same magnification the microstructure of the Fe-1.5 wt.% Mo alloy before (a) and after the 1st MS test run (b). The as-prepared sample (Figure 3a) has nanometric grain size and homogeneously distributed nano-porosity. The size of the pores is few nanometers. After the test run the sample has undergone the heating-cooling cycle in the temperature range $25\text{--}650^{\circ}\text{C}$ and its porosity has remarkably changed (Figure 3b). The average pore size has increased due to pore growth and coalescence, as clearly shown in Figure 3c, in particular by the detail displayed at higher magnification in Figure 3d. Here, a pore of large size is surrounded by smaller pores which are going to coalesce. Therefore, the decrease of $\sim 3\%$ of the dynamic modulus after the 1st test run can be explained by a decrease of density following pore growth and coalescence.

Moreover, the abrupt slope change of modulus observed at $\sim 430^{\circ}\text{C}$ suggests that growth and coalescence of the pores, which have a continuous evolution, may give rise to crack formation. In fact, cracks are not visible by an external inspection of the samples also at high magnification. The as-prepared material is hard and brittle, and contains a lot of pores separated by metallic ligaments with thickness of the order of few nanometers thus small cracks can originate from the tearing of these thin ligaments during heating to accommodate internal stresses.

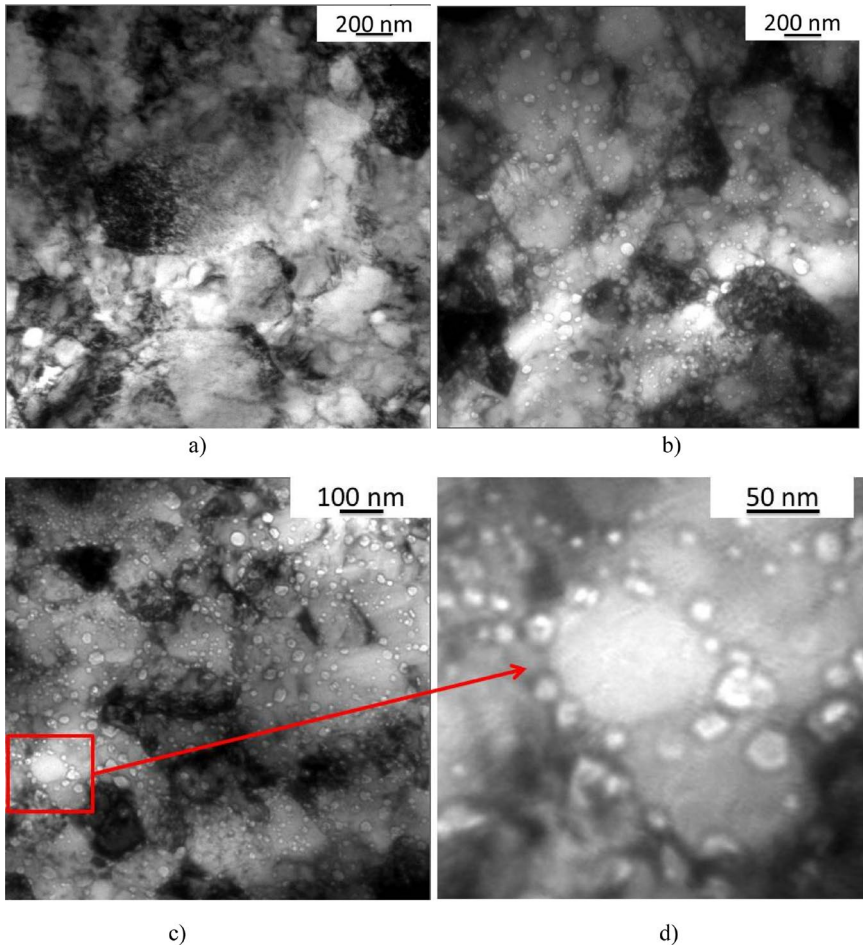


Figure 3. TEM micrographs of the sintered Fe-1.5 wt.% Mo alloy before (a) and after the 1st MS test run (b). The coalescence of some pores of small size is apparent in (c) and, in particular in the detail at higher magnification displayed in (d) showing a pore of large size is surrounded by smaller pores which are going to coalesce.

Figure 3b shows pores very close and aligned along the same direction: the rupture of the struts between the pores can easily form nanometric cracks. Indeed, crack formation reduces the effective sample thickness h and, according to Eq. (1), leads to a sudden decrease of the resonance frequency f . In fact, such apparent change of the modulus reveals the formation and growth of cracks of very small size, not otherwise detectable with other experimental techniques. The phenomenon was always observed above 400°C even if there is a certain randomness in terms of onset temperature and modulus variation in the different examined samples.

3.2 Pore closure in AlSi10Mg alloy manufactured by L-PBF

Plates (30 mm × 70 mm × 2 mm) of AlSi10Mg alloy have been manufactured by L-PBF technology using an EOS M290 machine and EOS powders with particles size is in the range 25–70 μm. The powder bed had a layer thickness of 30 μm and was selectively melted in Ar atmosphere with laser power of 370 W, scanning speed of 1300 mm/s and platform preheating at 80°C. The obtained density was $2.39 \pm 0.03 \text{ g/cm}^3$, namely ~ 90% of that of the bulk alloy. The microstructure of the material is described in detail in Giovagnoli et al. (2021) and Cabibbo, Montanari, Pola, Tocci, and Varone (2022). The rapid solidification, about 10^7 °C/s (Hooper, 2018), typical of this process leads to an extra-fine structure of Al cells surrounded by a network of Si particles. The Al phase exhibits networks of entangled dislocations which contribute to the high strength of the material in as-built condition. A drawback is represented by the porosity, consisting of micro-metric pores with irregular shape and spherical pores of nanometric size (Cabibbo et al., 2022). Given that the AlSi10Mg alloy is often used in automotive and aerospace industry also for high temperature applications, it is important to characterize its microstructure as a function of temperature for enhancing its use for high-temperature applications.

The reeds for MS experiments have been cut from the plates and tested without preliminary heat treatments. Successive test runs were carried out on the same sample. The measurements have been repeated on 15 different samples in the same experimental conditions and the results are highly reproducible with a substantial overlapping of the curves obtained in different experiments.

Figure 4 displays the anomalous trend of dynamic modulus in the 1st test run. Dynamic modulus is normalized to the value measured at room temperature in the 1st test run. Modulus vs. temperature curve is expected to have a monotonic decreasing trend owing to anharmonicity effect, however it starts to increase at ~ 170°C (point S), a maximum is observed at ~ 210°C (point F), then it decreases again. This behaviour is no more observed in the successive test runs and after the 1st run the modulus results to be increased of about 7% while the density of the material passes from 2.39 g/cm^3 (as-printed material) to 2.52 g/cm^3 . In the successive test runs the density substantially does not change.

A similar modulus behaviour was previously observed by us investigating a completely different material, namely sintered tungsten for applications as plasma facing material in future nuclear fusion reactors (Deodati, Donnini, Montanari, & Ucciardello, 2012). In that case the anomalous modulus trend was also accompanied by density increase due to the closure of sintering pores. To assess whether similar phenomena had the same

origin, the AlSi10Mg alloy has been examined by high-resolution Field Emission Scanning Electron Microscopy (FE-SEM) observations (ZeissTM Supra-40[®] field-emission gun scanning electron microscope) after conventional metallographic preparation, namely mechanical polishing and etching with Keller reagent at room temperature for 20–30 s.

Figure 5 shows the structure of the alloy in as-printed condition (a) and after heating up to 210°C (point F in Figure 4). In these MS experiments the 1st run was interrupted when the samples reached the temperature corresponding to the anomaly finish and immediately cooled down to avoid that the heating at higher temperature can modify the microstructure and, in particular, the porosity.

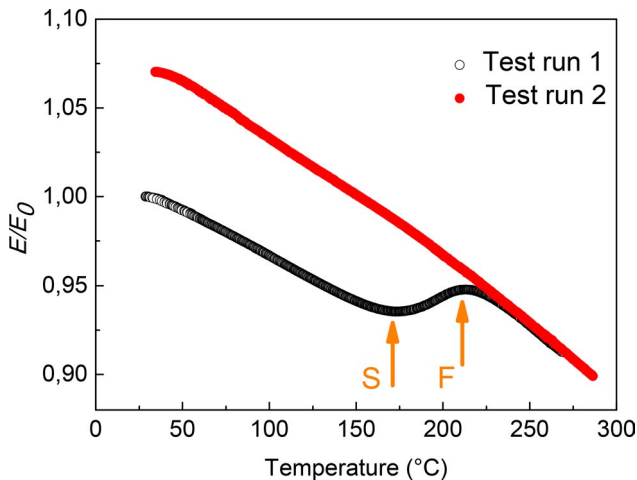


Figure 4. Dynamic modulus E vs. temperature of the AlSi10Mg alloy manufactured by L-PBF measured in two successive test runs. The values of E are normalized to the value E_0 measured at room temperature in the 1st test run. Arrows indicate the temperature range where anomalous modulus behaviour starts (S) and finishes (F).

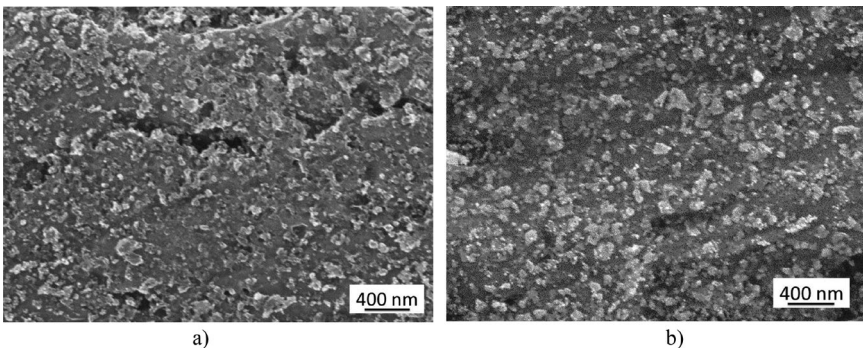


Figure 5. FE-SEM micrographs of as-printed AlSi10Mg alloy before (a) and after a MS test run with heating up to 210°C (b).

The FE-SEM micrographs at high magnification show relevant differences of porosity before (a) and after (b) the heating up to 210°C, namely the nano-pores present in the as-printed alloy disappear after heating. This is a clear evidence that the modulus anomaly is due to a densification process of the alloy that takes place in the temperature range 170–210°C involving the closure of the smallest pores, of nanometric size. It is noteworthy that the pores of micro-metric size are still present in the heated samples, most likely owing to oxidation of internal pore surfaces or presence of gas inside the pores.

3.3 No change of porosity in the Ti6Al4V alloy manufactured by L-PBF

Ti6Al4V alloy was manufactured by L-PBF by using the same process parameters used for Al10SiMg and described in the previous section. Unmolten powder particles have been observed on the surface of the samples (see [Figure 6](#)) thus it has been mechanically polished before the MS tests. Porosity consists of some pores of large size, of the order of 40–50 µm, such that displayed by [Figure 6](#).

MS tests were performed by varying the temperature from room temperature (25°C) up to 820°C. As shown in [Figure 7](#), in this temperature range dynamic modulus does not exhibit the anomalous behaviour observed in the case of AlSi10Mg: it monotonically decreases as temperature increases (there are only large pores). On the other hand, FE-SEM observations do not show significant porosity variations after MS test runs.

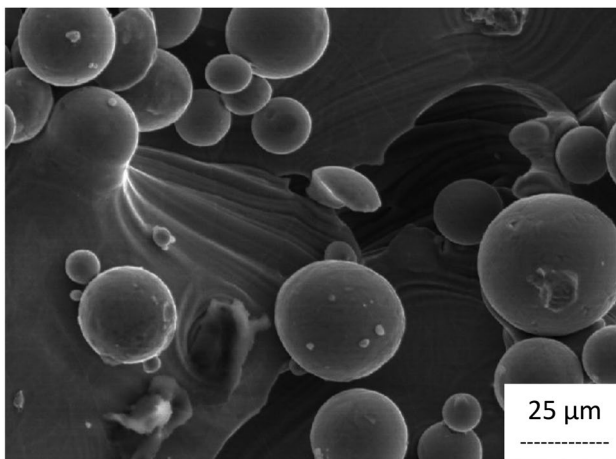


Figure 6. Ti6Al4V alloy manufactured by L-PBF exhibits few pores of large size (~40 µm).

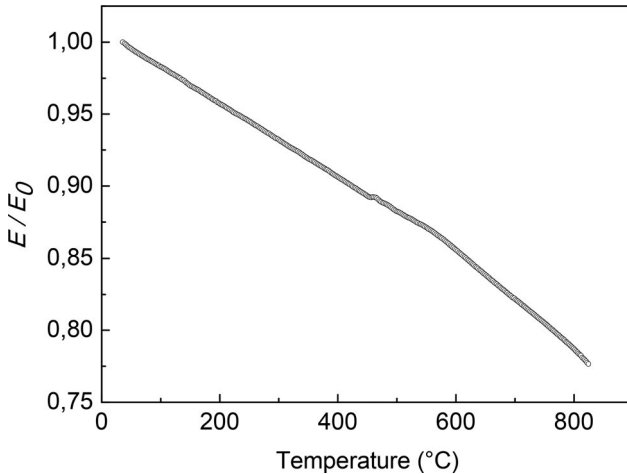


Figure 7. Dynamic modulus E vs. temperature of the Ti6Al4V alloy manufactured by L-PBF. The values of E are normalized to the value E_0 measured at room temperature.

4. Conclusions

In this work three cases of possible pore structure evolution in different metallic alloys have been examined: (i) growth and coalescence of pores, (ii) closure of pores of nanometric size and (iii) no change of porosity.

The results of these experiments highlight how dynamic modulus measurements can be successfully employed for a direct monitoring of porosity variations during heating. The technique is quite sensitive and allows to identify the temperature range where pore evolution takes place providing information useful to orientate heat treatments of porous materials.

Disclosure statement

No potential conflict of interest was reported by the authors.

Notes on contributors

Marcello Cabibbo Full Professor of Metallurgy at Polytechnic University of Marche. The main research topics are: (i) high temperature mechanical behavior of light alloys and steels, (ii) characteristics of thin coatings, and (iii) micro-structural characterization of light alloys, steels, cast iron, superalloys and Cu alloys.

Chiara de Crescenzo Post-doc at the University of Rome Tor Vergata. The main research topics are: (i) 3D additive manufactured lattice structures, (ii) evaluation and prediction of surface roughness in additive manufactured parts, and (iii) nickel alloys welding and repairing by high density energy processes.

Roberto Montanari Full Professor of Metallurgy at the University of Rome Tor Vergata. The main research topics are: (i) structure and micro-chemistry of liquid metals, (ii) structural and plasma facing materials for nuclear fusion reactors, (iii) biodegradable alloys for medical applications, and (iv) microstructure and properties of 3D printed alloys.

Maria Richetta Associate Professor of Design and Methods of Industrial Engineering. The main research topics are: (i) lattice structures and topological optimization, (ii) plasma facing materials for nuclear fusion reactors, (iii) structure and characteristics of LDH coatings for medical applications, and (iv) microstructure and properties of 3D printed alloys.

Alessandra Varone Associate Professor of Metallurgy at the University of Rome Tor Vergata. The main research topics are: (i) structure and micro-chemistry of liquid metals, (ii) structural and plasma facing materials for nuclear fusion reactors, (iii) biodegradable alloys for medical applications, and (iv) microstructure and properties of 3D printed alloys.

References

- Alberici, S., Montanari, R., & Tata, M. E. (2000). H induced C-Cr associate redistribution in MANET steel. *Journal of Alloys and Compounds*, 310(1–2), 209–213. [https://doi.org/10.1016/S0925-8388\(00\)01027-6](https://doi.org/10.1016/S0925-8388(00)01027-6)
- Amadori, S., Bonetti, E., Deodati, P., Donnini, R., Montanari, R., Pasquini, L., & Testani, C. (2009). Low temperature damping behaviour of Ti6Al4V + SiC_f composite. *Materials Science and Engineering: A*, 521–522, 340–342. <https://doi.org/10.1016/j.msea.2008.09.156>
- Amadori, S., Campari, E. G., Fiorini, A. L., Montanari, R., Pasquini, L., Savini, L., & Bonetti, E. (2006). Automated resonant vibrating reed analyzer apparatus for a non destructive characterization of materials for industrial applications. *Materials Science and Engineering: A*, 442(1–2), 543–546. <https://doi.org/10.1016/j.msea.2006.02.210>
- Banhart, J. (2001). Manufacture, characterisation and application of cellular metals and metal foams. *Progress in Materials Science*, 46(6), 559–632. [https://doi.org/10.1016/S0079-6425\(00\)00002-5](https://doi.org/10.1016/S0079-6425(00)00002-5)
- Bennett, T. D., Coudert, F. X., James, S. L., & Cooper, A. I. (2021). The changing state of porous materials. *Nature Materials*, 20(9), 1179–1187. <https://doi.org/10.1038/s41563-021-00957-w>
- Blanter, M. S., Golovin, I. S., Neuhäuser, H., & Sinning, H.-R. (2007). *Internal friction in metallic materials*. Springer Series in Materials Science. Berlin Heidelberg: Springer Verlag ISBN 10: 3642088252 ISBN 13: 9783642088254
- Boccaccini, A. R., Ondracek, G., Mazilu, P., & Windelberg, D. (1993). On the effective Young's modulus of elasticity for porous materials: Microstructure modelling and comparison between calculated and experimental values. *Journal of the Mechanical Behavior of Materials*, 4(2), 119–128. <https://doi.org/10.1515/JMBM.1993.4.2.119>
- Bocchini, G. F., Montanari, R., & Varone, A. (2013). Influence of probe test orientation, sintering degree and morphological anisotropy of porosity on the Young's modulus of homogeneous sintered steel. In *Proceedings of the EPMA*, Gothenburg, Sweden.

- Bolli, E., Fava, A., Ferro, P., Kaciulis, S., Mezzi, A., Montanari, R., & Varone, A. (2020). Cr segregation and impact fracture in a martensitic stainless steel. *Coatings*, 10(9), 843. <https://doi.org/10.3390/coatings10090843>
- Bonetti, E., Cabibbo, M., Campari, E. G., & Montanari, R. (2021). Correlation between anelastic response and microstructure of 5N-Al thin foils. *Journal of Alloys and Compounds*, 872, 159693. <https://doi.org/10.1016/j.jallcom.2021.159693>
- Bonetti, E., Montanari, R., Testani, C., & Valdré, G. (2000). Irreversible transformation in as-cast FeAl B2-ordered alloy obtained by melt spinning. *Journal of Materials Research*, 15(3), 659–664. <https://doi.org/10.1557/JMR.2000.0098>
- Cabibbo, M., Montanari, R., Pola, A., Tocci, M., & Varone, A. (2022). Mechanical spectroscopy study of as-cast and additive manufactured AlSi10Mg. *Journal of Alloys and Compounds*, 914, 165361. <https://doi.org/10.1016/j.jallcom.2022.165361>
- Campari, E. G., Amadori, S., Bonetti, E., Berti, R., & Montanari, R. (2019). Anelastic behaviour of small dimensioned aluminum. *Metals*, 9(5), 549. <https://doi.org/10.3390/met9050549>
- Chen, Z., Wang, X., Giuliani, F., & Atkinson, A. (2015). Microstructural characteristics and elastic modulus of porous solids. *Acta Materialia*, 89, 268–277. <https://doi.org/10.1016/j.actamat.2015.02.014>
- Deodati, P., Donnini, R., Montanari, R., & Testani, C. (2009). High temperature damping behaviour of Ti6Al4V + SiC_f composite. *Materials Science and Engineering: A*, 521–522, 318–321. <https://doi.org/10.1016/j.msea.2008.09.109>
- Deodati, P., Donnini, R., Montanari, R., & Ucciardello, N. (2012). Microstructural investigation on tungsten for applications in future nuclear fusion reactors. *Materials Science Forum*, 706–709, 835–840. <https://doi.org/10.4028/www.scientific.net/MSF.706-709.835>
- Deodati, P., Montanari, R., Tassa, O., & Ucciardello, N. (2009). Single crystal PWA 1483 superalloy: Dislocation rearrangement and damping phenomena. *Materials Science and Engineering: A*, 521–522, 102–105. <https://doi.org/10.1016/j.msea.2008.09.107>
- Dukhan, N., Chen-Wiegart, Y. K., Paz y Puente, A., Erdeniz, D., & Dunand, D. C. (2020). Porous metals: From nano to macro. *Journal of Materials Research*, 35(19), 2529–2534. <https://doi.org/10.1557/jmr.2020.282>
- Eudier, M. (1962). The mechanical properties of sintered low-alloy steels. *Powder Metallurgy*, 5(9), 278–290. <https://doi.org/10.1179/pom.1962.5.9.005>
- Fava, A., Montanari, R., Richetta, M., Testani, C., & Varone, A. (2018). Analysis of strengthening mechanisms in nano-ODS steel depending on preparation route. *Journal of Material Sciences & Engineering*, 7(4), 1000474. doi:10.4172/2169-0022.1000474
- Gibson, L. J., & Ashby, M. F. (1989). Cellular solids. In *Structure and properties* (2nd ed.). Cambridge, UK: Cambridge University Press. <https://doi.org/10.1017/CBO9781139878326>
- Giovagnoli, M., Tocci, M., Fortini, A., Merlin, M., Ferroni, M., Migliori, A., & Pola, A. (2021). Effect of different heat-treatment routes on the impact properties of an additively manufactured AlSi10Mg alloy. *Materials Science and Engineering: A*, 802, 140671. <https://doi.org/10.1016/j.msea.2020.140671>
- Gondi, P., & Montanari, R. (1992). On the Cr distribution in MANET steel. *Physica Status Solidi (a)*, 131(2), 465–480. <https://doi.org/10.1002/pssa.2211310221>

- Gondi, P., & Montanari, R. (1994). Q^{-1} spectra connected with C under solute atom interaction. *Journal of Alloys and Compounds*, 211–212, 33–36. [https://doi.org/10.1016/0925-8388\(94\)90441-3](https://doi.org/10.1016/0925-8388(94)90441-3)
- Gupta, R., Gondi, P., Montanari, R., Principi, G., & Tata, M. E. (1997). Internal friction and Mössbauer study of C-Cr associates in MANET steel. *Journal of Materials Research*, 12(2), 296–299. <https://doi.org/10.1557/JMR.1997.0038>
- Hooper, P. A. (2018). Melt pool temperature and cooling rates in laser powder bed fusion. *Additive Manufacturing*, 22, 548–559. doi:10.1016/j.addma.2018.05.032
- Jafari, D., van Alphen, K. J. H., Geurts, B. J., Wits, W. W., Cordova Gonzalez, L., Vaneker, T. H. J., ... Gibson, I. (2020). Porous materials additively manufactured at low energy: Single-layer manufacturing and characterization. *Materials & Design*, 191, 108654. <https://doi.org/10.1016/j.matdes.2020.108654>
- Kovačik, J. (1999). Correlation between Young's modulus and porosity in porous materials. *Journal of Materials Science Letters*, 18(13), 1007–1010. <https://doi.org/10.1023/A:1006669914946>
- Manoylov, A. V., Borodich, F. M., Evans, H. P. (2013). Modelling of elastic properties of sintered porous materials. *Proceedings of the Royal Society A: Mathematical, Physical and Engineering Sciences*, 469, 20120689. <https://doi.org/10.1098/rspa.2012.0689>
- Michailidis, N., Stergioudi, F., Omar, H., Papadopoulos, D. P., & Tsipas, D. N. (2011). Experimental and FEM analysis of the material response of porous metals imposed to mechanical loading. *Colloids and Surfaces A: Physicochemical and Engineering Aspects*, 382(1–3), 124–131. <https://doi.org/10.1016/j.colsurfa.2010.12.017>
- Michailidis, N., Tsouknidas, A., Lefebvre, L.-P., Hipke, T., & Kanetake, N. (2014). Production, characterization, and applications of porous materials. *Advances in Materials Science and Engineering*, 2014, 1–2. <https://doi.org/10.1155/2014/263129>
- Mitchell, M. R., Link, R. E., Iacovone, B., Libardi, S., Molinari, A., Zadra, M., ... Plini, P. (2008). FIMEC tests on SPS sintered FeMo nanostructured alloys. *Journal of Testing and Evaluation*, 36(5), 101365. <https://doi.org/10.1520/JTE101365>
- Montanari, R., & Varone, A. (2012). Mechanical spectroscopy investigation of liquid Pb-Bi alloys. *Solid State Phenomena*, 184, 434–439. <https://doi.org/10.4028/www.scientific.net/SSP.184.434>
- Montanari, R., & Varone, A. (2015). Synergic Role of Self-interstitials and Vacancies in Indium Melting. *Metals*, 5(2), 1061–1072. <https://doi.org/10.3390/met5021061>
- Nakajima, H. (2007). Fabrication, properties and application of porous metals with directional pores. *Progress in Materials Science*, 52 (7), 1091–1173. <https://doi.org/10.1016/j.pmatsci.2006.09.001>
- Nowick, A. S., & Berry, B. S. (1972). *Anelastic relaxation in crystalline solids*. New York, NY; London, UK: Academic Press. <https://doi.org/10.1016/B978-0-12-522650-9.X5001-0>
- Pabst, W., & Gregorová, E. (2014). Young's modulus of isotropic porous materials with spheroidal pores. *Journal of the European Ceramic Society*, 34(13), 3195–3207. <https://doi.org/10.1016/j.jeurceramsoc.2014.04.009>
- Richetta, M., & Varone, A. (2020). A focus on dynamic modulus: Effects of external and internal morphological features. *Metals*, 11(1), 40. <https://doi.org/10.3390/met11010040>

- Sousa, L., Pereira, L., Montes-González, D., Ramos, D., Amado-Mendes, P., Barrigón-Morillas, J. M., & Godinho, L. (2023). Experimental analysis and simulation of a porous absorbing layer for noise barriers. *Applied Sciences*, 13(4), 2638. <https://doi.org/10.3390/app13042638>
- Suzuki, A., Kosugi, N., Takata, N., & Kobashi, M. (2020). Microstructure and compressive properties of porous hybrid materials consisting of ductile Al/Ti and brittle Al₃Ti phases fabricated by reaction sintering with space holder. *Materials Science and Engineering: A*, 776, 139000. <https://doi.org/10.1016/j.msea.2020.139000>
- Torquato, S. (2002). *Random heterogeneous materials – Microstructure and macroscopic properties* (pp. 437–563). New York: Springer. doi:10.1115/1.1483342
- Vijayan, S., Anna Dilfi, K. F., & Venkatachalapathy, S. (2022). Porous metals. In A. Uthaman, S. Thomas, T. Li, & H. Maria (Eds.), *Advanced functional porous materials. engineering materials*. Switzerland: Springer Nature. https://doi.org/10.1007/978-3-030-85397-6_15
- Yang, X. Y., Chen, L. H., Li, Y., Rooke, J. C., Sanchez, C., & Su, B. L. (2017). Hierarchically porous materials: Synthesis strategies and structure design. *Chemical Society Reviews*, 46(2), 481–558. <https://doi.org/10.1039/C6CS00829A>